Static- and fabrication-aware segmented concrete shells made of post-tensioned precast flat tiles

Francesco Laccone[1][0000−0002−3787−7215], Sandro Menicagli[2], Paolo Cignoni[1][0000−0002−2686−8567], and Luigi Malomo[1][0000−0001−7892−894X]

[1] ISTI - CNR, via G. Moruzzi 1, Pisa, Italy
[2] University of Pisa, Lungarno Pacinotti 43, Pisa, Italy
francesco.laccone@isti.cnr.it

Abstract. This paper introduces a novel structural concept for freeform shells, in which the shape is decomposed into flat tiles to be assembled sequentially with the help of falseworks. Once the structure is completed, the tiles are post-tensioned to minimize the tension forces and avoid detachment. The entire design process, from an input shape to fabrication, is managed by an automatic pipeline. The input shape is segmented into a field-aligned quad mesh, computed from the principal stress of the thin shell. The flat tiles are obtained by extruding each face along the normal of the best-fitting plane per face. The contact between adjacent tiles is ensured only at their edge midpoints so the forces can mainly flow along the cross directions. The best configuration of cable paths and pre-loads is found by solving a constrained optimization problem exploiting a reduced beam model of the shell. All tiles can be prefabricated in the shop with an adaptable and reusable molding system. Once the structure is completed, the top surface is finally completed with an in situ cast that fills the gaps and activates the entire shell behavior. In contrast, the bottom surface maintains its jagged aesthetics.

Keywords: Concrete · Freeform surfaces · Computational design · Optimization · Digital fabrication.

1 Concrete shells: fabrication and design

The design of freeform concrete shells has regained popularity in recent times thanks to computational tools, which allow manipulating and exploring complex shapes interactively. Also, novel digital fabrication techniques shorten the distance between digital shape and fabricated structure [5, 8]. However, in most cases, the actual fabrication of concrete shells, even on a small scale, still poses challenges of feasibility and cost.

The success of concrete shells lies in their ability to develop membrane behavior through their shape and the possibility of the fluid material being cast in any required geometry efficiently. Forming appropriate 3D shells requires pre-formed molds. Rigid continuous and dense formworks have made large and accurate concrete shells feasible since ancient times, from simple barrel vaults to form-found

Fig. 1. Conceptual view with technical details of our concrete shell: the shape is segmented into flat tiles that are jointed at the midpoint of the edges and post-tensioned; the outer surface is finished with wire patches and in situ casting.

shapes. While in the past formworks were realized by skilled craftsmen that cut and bent wood or metal panels, additive and subtractive fabrication nowadays supports their realization as custom single-use pieces to be assembled. However, these are labor-intensive and costly technology, mainly because of the limited reusing degree. The use of dense formworks has gradually decreased in favor of simpler and faster construction processes. An alternative concept is the stay-in-place formwork, which provides knitted, wire mesh, bricks or other flexible/solid patches forming the mold and the surface finishing of the completed shell. In all these cases, concrete is cast or sprayed on site and the resulting structure is monolithic with few or no joints.

On the other hand, advances in manufacturing and analysis have provided new concepts based on segmentation into panels or tiles, which may be flat, single or double-curved. The molds for these tiles are fabricable with numerically controlled machines out of different materials. However, a single mold produces a unique element leading to a low prefabrication rate, especially in the case of variable curvature and unavoidable waste production. Flexible formworks are introduced as a viable alternative process to adapt their shape and form a variety of molds [1]. Segmented shells made of precast parts need to be assembled on site with the inherent formation of joints, which have to be stiff and resistant to not disturb the development of shell action. In this paper, we combine the advantages of segmentation for prefabrication in the shop with the continuity provided by a final on-site casting as in Fig. 1. Such an approach was adopted in bold structural architectures from the past, such as the ribbed shell of Palazzetto dello Sport in Rome by Nervi. In the Nervi building system, curved

precast ferrocement panels supported by falsework are finally finished with in situ concrete. Flat prismatic tiles are the best manufacturing option because they can be produced off-site with a master mold to be reused several times. High efficiency, precision and economy can be achieved. Moreover, the spreading of digital fabrication has made design variations for mass customization possible and cheap. However, freeform shapes can not be naturally split into flat tiles [2], and any discretization introduces weak lines that may alter the load path [6]. Therefore, we introduce a method for decomposing freeform shells into prismatic tiles, which are aligned to the principal stress directions for structural efficiency and flat for easy fabrication. These tiles share edge midpoint contact and are post-tensioned to favor a compression-only behavior. We develop an automatic pipeline that starts from a generic freeform shape and delivers tiles to the factory. We optimize the set of cable and their pre-load. We address all aspects of design and fabrication. Eventually the shell is completed with on-site casting.

2 Concept and geometry of segmented shells

We propose a novel structural concept for freeform shells, in which the shape is decomposed into flat quadrilateral tiles to form right prisms (with sides and faces forming 90° angles), touching each other at the midpoint of their edges. The segmented shell is efficient as long as all tiles remain in touch, i.e. the shell is compressed. So, once assembled, the tiles are post-tensioned to minimize the resulting tension on the structure under service load. The outer surface is finally completed with an in situ cast that fills the gaps and activates the shell behavior. The bottom surface presents a jagged aesthetic due to gaps and misalignment at the seams.

Our pipeline to deliver the tiles is shown in Fig. 2. We convert the input shape (Fig. 2a) into a thin shell. Then, we run a static analysis under uniformly-distributed load, whose principal stress lines (Fig. 2b) yield a cross-field used for producing a quad mesh (Fig. 2c). The obtained quad faces can have any curvature, however, we project each face on its best-fitting plane, obtaining a disjointed mesh of planar quad faces (Fig. 2d). The latter is very close to the checkerboard mesh associated with the starting quad mesh. The checkerboard mesh is a derivation of the Varignon theorem: a polygon (i.e., Varignon polygon)

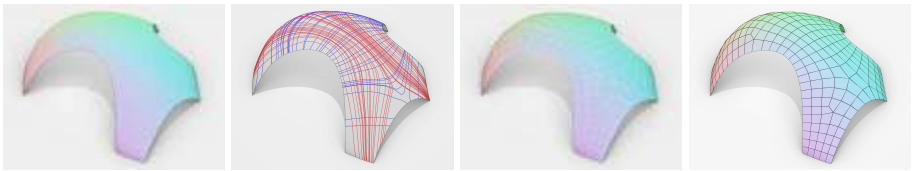

(a) (b) (c) (d)

Fig. 2. Pipeline: (a) input shape; (b) stress isolines from the continuum thin shell; (c) field-driven quad mesh; (d) disjointed flat tiles.

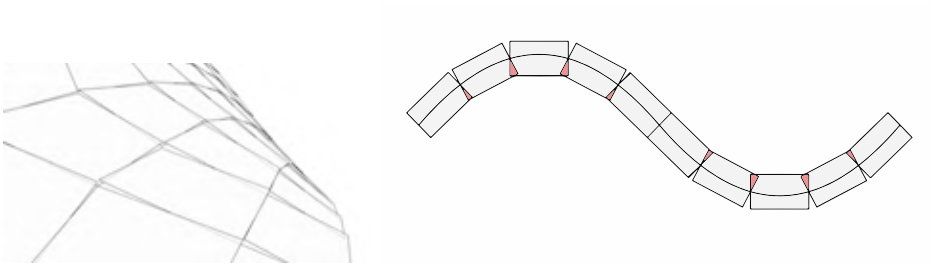

(a) (b)

Fig. 3. (a) Flattening individual faces of a quad mesh on the best fitting plane through the vertices, obtaining a disjointed quad mesh; (b) the extrusion along the flat face normal produces overlaps and gaps among the tiles.

formed by the edge midpoint subdivision of a control face (quad in our case), which is planar whether the starting face is planar or not [7]. The resulting checkerboard mesh has 'black' planar rhomboid faces and arbitrary nonplanar 'white' faces. The closest points of two adjacent tiles are their edge midpoints as in Fig. 3a, which will be equipped with joints. Therefore, inter-tile forces can only flow through their edges' midpoint. Since the tiles are aligned with the principal stress directions, each tile is stressed mainly along its cross directions.

Practically, the tiles have a proper thickness, and the extrusion of the disjointed flat faces along their normals produces overlaps and gaps (Fig. 3b), which are a function of curvature and size of the tile (both edge size and thickness). While gaps are acceptable to a certain extent, a material intersections are not feasible. We start from the simple idea of having gaps only and extruding the planar face, which would have minimized the gaps. Working in the discrete prisms setup (as in Fig. 3b) would have required solving a complex iterative Boolean intersection.

Instead, we compute the mesh offset for both shell sides (yellow and light blue meshes in Fig. 4), which produces, in the general case, non-parallel and nonplanar faces. Then, for each face of both offset meshes, we project the vertices on the best-fitting plane and compute the maximum intersection area of the two projected quads (Fig. 4). This operation leads to the minimum projected quad in the more straightforward case, i.e., in convex or concave areas. In contrast, in the general case, the intersection area can have multiple vertices (red polygon in Fig. 4) To conservatively restore the initial vertex number, vertices with incident segments closest to colinear are culled (green polygon). This straightforward approach remarkably preserves the number of vertices per face and is dependent on the selected thickness of the shell: the smaller, the closer the tiles.

Cables lie by design on the mid-surface of the shell to exert compression globally once post-tensioned. We build a large and distributed set of candidate cables, from which choosing the optimal subset within an optimization problem (Sec. 3). Candidate paths are found by chaining the segments linking pairs of opposite edge midpoints on a tile (Fig. 5a). We discard paths that do not end

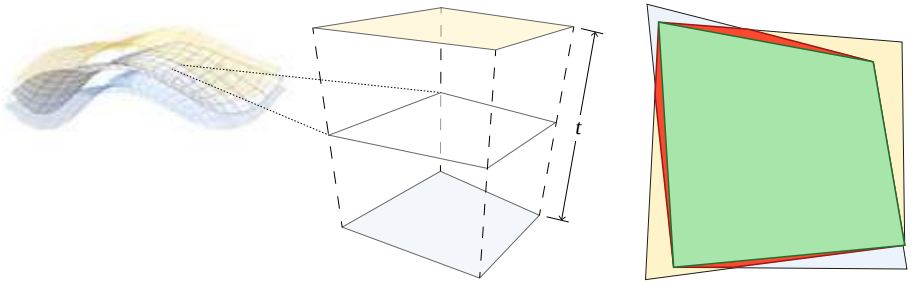

Fig. 4. Removing overlaps: the offset meshes are projected on a flat tile (extrusion thickness t is exaggerated for visualization purposes only).

on the boundary (closed loops) or paths with significant kinks ($\alpha < \textit{threshold}$ in Fig. 5a), to avoid localized shear on the surface (Fig. 5).

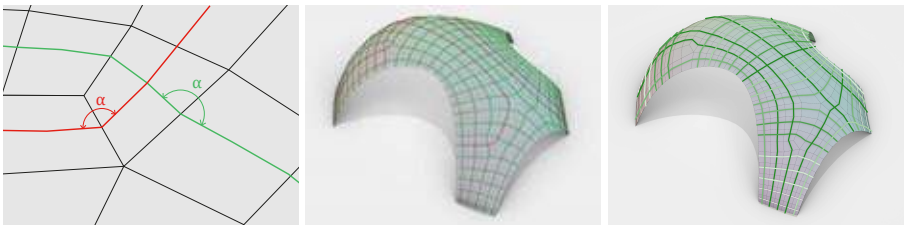

(a) (b) (c)

Fig. 5. Selection of cable paths: (a) closeup on candidate cable path (green) and discarded path (red); (b) all candidate and discarded paths; (c) selected cables after the optimization as per Eq. (1) (the darker, the higher the pre-load).

3 Structural design, modeling and optimization

In the disjointed mesh, by design, the adjacent faces come (almost) in touch at the midpoints of each tile edge. These points are affected by a delicate structural task of transferring forces from tile to tile. C-profile steel segments are incorporated during the tile casting to avoid any possible local failure due to contacts and localized loads (Fig. 6a). These steel components serve two other functions: (a) restraining the ducts during the tiles' fabrication and (b) accommodating the connectors (bolts and plates) during the assembly of the shell. All tiles can be prefabricated in the shop employing an adaptable and reusable molding system. The mold walls can be altered to form any angle and edge length (Fig. 6b). Also, singular tiles, like triangles and polygons, can be formed with this system.

(a) (b)

Fig. 6. (a) Detailed design of the prismatic tile with embedded cables' ducts and steel C-profile segments at the contact interfaces. (b) Adaptable molding system.

Since the mesh faces are aligned with the principal stress directions, and the adopted detail enforces punctual force transfer, the tiles show a predominant strut-and-tie behavior along the two crossing directions (the tile shear is negligible). Therefore, the structure can be modeled as a grid of beams for optimization purposes (Fig. 7). Each cable is a polyline changing direction from tile to tile, overlapping a subset of the beams. It pre-loads the shell (namely the grid of beams) primarily at the kinks. We model the effect of the j-th cable on the structure as an equivalent load F_j acting at the cable kinks. Assuming for simplicity to be in a linear setup, the beams' internal forces produced by each F_j can be superimposed on the results of a linear analysis under service load.

Furthermore, because of the linearity, the cable effect can be scaled by a factor, i.e., its pre-load p_j. Similarly to [4], we select appropriate cables and their accompanying pre-load by solving a constrained minimization problem:

$$min(\sum f_t(p_j)) \tag{1}$$

$$s.t.\ \ 0 \leq p_j \leq p_{max} \tag{2}$$

In which $\sum f_t$ is the sum among all beams of tension forces only. All configurations (service load scenario and individual cables' equivalent-load scenarios) are pre-computed and linearly superimposed to find the minimum of the objective function. The equilibrium of the structure holds as a superimposition of multiple equilibrium conditions. Eq. (2) defines a limitation on the allowable pre-stress on each cable.

4 Results and discussion

We tested our pipeline on a quasi-membrane shape with large openings and non-trivial structural behavior. The service load adopted in the optimization is the sum of the structural weight and $\gamma_q q_k = 1.5 \times 0.5\ kN/m^2$. The shape has a bounding box of $15.0 \times 13.0 \times 5.0\ m$ for a total projected area of $110\ m^2$, 269 prismatic faces of average edge length of $0.70\ m$ and $t = 0.06\ m$ thickness. Our reduced model adopts beams cross sections equal to the web of the steel C-profile

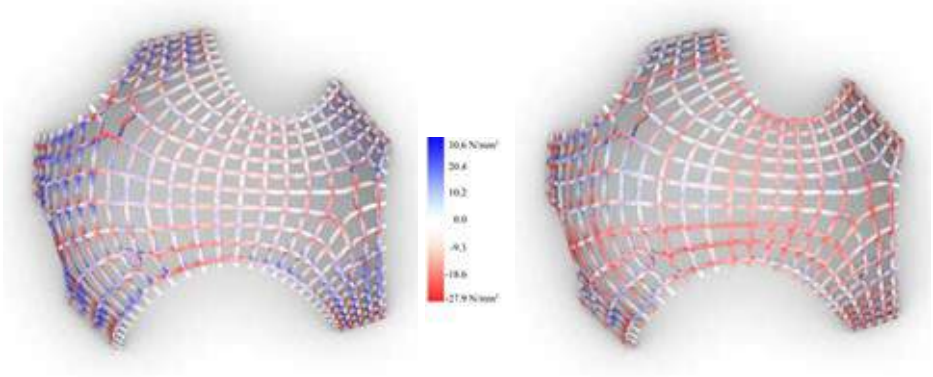

(a) (b)

Fig. 7. Stress in the reduced model linear analysis: (a) starting shell under service load; (b) shell deploying optimized cables.

($0.06 \times 0.18\ m$) and C28/35 concrete as material. The reduced model analysis at the starting condition (with no cables, Fig. 7a) confirms the effectiveness of the meshing and model reduction strategy, showing low bending moments and shear forces.

The entire cable set comprises 44 cables. 32 of them are selected in the optimization (see Fig. 5c). We adopt a 8 mm diameter cables for an allowable pre-stress $p_{max} = 30\ kN$. The optimization problem of Eqs. (1) and (2) is solved using two algorithms from the NLopt library [3] in sequence: CRS2, for global evolutionary search, and BOBYQA, a derivative-free local refinement. The optimization leads to an significant reduction of the tension on the elements (Fig. 7b) and an overall improvement of the shell statics (Tab. 1).

Table 1. Analysis results from the reduced model before (start) and after the optimization (opt).

	Unit	Value
Max displacement (start)	m	0.02
Max compression force f_c (start)	kN	35.30
Max tension force f_t (start)	kN	8.06
Sum of tension forces $\sum f_t$ (start)	kN	**582.54**
Max displacement (opt)	m	0.02
Max compression force f_c (opt)	kN	82.96
Max tension force f_t (opt)	kN	6.86
Sum of tension forces $\sum f_t$ (opt)	kN	**78.07**

The pipeline results in a labeled set of prismatic tiles and cable segments, which are easily fabricable. The assembly (Fig. 8) requires falseworks to fulfill

the stability of the tiles once they are sequentially moved to their target position. The shape curvature and the anchoring of connectors between the tiles gradually favor the formation of stable patches. Similarly, the connectors can transfer both tension and compression once the assembly is completed. The cables can be pushed into the ducts and post-tensioned from the boundary up to the desired pre-load (Fig. 8c). We tested the feasibility of the assembly routine on a scale model made of 3D-printed flat tiles as in Fig. 9.

To add more redundancy and to fill the gaps between the tiles while providing a finishing of the structure, an in situ cast can be arranged on the outer surface of the structure. This cast embeds a fiberglass or steel wire mesh. As a last step of our pipeline, we found a clustering method for the wire mesh (Fig. 10). The target double-curved surface is decomposed into developable flat patches having specific shapes and cuts so that these patches can be laid on the shell without significant distortions or wrinkles. As an additional fabrication constraint, we also require the patches to fit into the size of commercially-available sheets of material. Simultaneously, the ducts can be grouted so that the cables can be effectively coupled with concrete and prevent steel corrosion.

5 Conclusions

In this paper, we presented a design method that is an alternative to traditional concrete shells in both mechanics and fabrication and is expected to offer cost savings. We introduced a new structural concept and an automated pipeline to deliver segmented shells made of prismatic tiles, which are easily fabricable and can be handily assemble to form a proper structure. To guarantee discrete tiles to develop a suitable load-bearing scheme, we adopt a meshing aligned to the principal stress directions, and to avoid detachment, we post-tension the tiles utilizing optimal embedded cables.

The method works for complex shapes and can handle several design variables to tune the stiffness and strength of the final solution. However, the efficiency of this system is higher in areas of double curvature where the geometry of the shape and the post-tensioning load provide the best contribution. Several topics deserve further research efforts. On the structural side, for instance, several

(a) (b) (c)

Fig. 8. Assembly: (a) laying the tiles starting from the supports; (b) sequential assembly with falseworks; (c) completion and post-tensioning.

Fig. 9. Assembly steps of a 3D printed demonstrator.

redundancy layers are designed (post-tensioning, connectors, completion cast). However, their contribution to the statics and stability is to be investigated. We reasonably believe that the structural model adopted, as a grid of beams in accordance with the meshing and load transfer mechanism, could represent a lower-bound solution. Actually the structural response must be evaluated with more advanced simulations and testing. On the practical side, the essential topic is investigating fabrication tolerances and the effect of the size of the gaps between the tiles. Eventually, production and physical experiments could provide relevant insight to improve the design method.

References

1. Hawkins, W.J., Herrmann, M., Ibell, T.J., Kromoser, B., Michaelski, A., Orr, J.J., Pedreschi, R., Pronk, A., Schipper, H.R., Shepherd, P., Veenendaal, D., Wansdronk, R., West, M.: Flexible formwork technologies – a state of the art review. Structural Concrete **17**(6), 911–935 (2016). https://doi.org/https://doi.org/10.1002/suco.201600117
2. Jiang, C., Wang, C., Tellier, X., Wallner, J., Pottmann, H.: Planar panels and planar supporting beams in architectural structures. ACM Transactions on Graphics (2022). https://doi.org/10.1145/3561050, http://hdl.handle.net/10754/680820
3. Johnson, S.G.: The NLopt nonlinear-optimization package (Dec 2021), https://github.com/stevengj/nlopt
4. Laccone, F., Malomo, L., Froli, M., Cignoni, P., Pietroni, N.: Automatic Design of Cable-Tensioned Glass Shells. Computer Graphics Forum **39**(1), 260–273 (2020). https://doi.org/https://doi.org/10.1111/cgf.13801

(a) (b)

Fig. 10. Minimum distortion patches of wire mesh to lay on the top face of the shell: (a) developable patches; (b) flat sheets of material.

5. Li, W., Lin, X., Bao, D.W., Xie, Y.M.: A review of formwork systems for modern concrete construction. Structures **38**, 52–63 (2022). https://doi.org/https://doi.org/10.1016/j.istruc.2022.01.089
6. Oval, R., Rippmann, M., Mesnil, R., Van Mele, T., Baverel, O., Block, P.: Feature-based topology finding of patterns for shell structures. Automation in Construction **103**, 185–201 (2019). https://doi.org/https://doi.org/10.1016/j.autcon.2019.02.008, https://www.sciencedirect.com/science/article/pii/S0926580518304321
7. Peng, C.H., Jiang, C., Wonka, P., Pottmann, H.: Checkerboard Patterns with Black Rectangles. ACM Trans. Graph. **38**(6) (nov 2019). https://doi.org/10.1145/3355089.3356514, https://doi.org/10.1145/3355089.3356514
8. Wangler, T., Lloret, E., Reiter, L., Hack, N., Gramazio, F., Kohler, M., Bernhard, M., Dillenburger, B., Buchli, J., Roussel, N., et al.: Digital concrete: opportunities and challenges. RILEM Technical Letters **1**, 67–75 (2016)